Hypothalamic deep brain stimulation as a strategy to manage anxiety disorders

Han-Tao Li[a,b] [ID], Dane C. Donegan[b], Daria Peleg-Raibstein[b,c,d,1,2], and Denis Burdakov[b,c,d,1,2] [ID]

Fear is essential for survival, but excessive anxiety behavior is debilitating. Anxiety disorders affecting millions of people are a global health problem, where new therapies and targets are much needed. Deep brain stimulation (DBS) is established as a therapy in several neurological disorders, but is underexplored in anxiety disorders. The lateral hypothalamus (LH) has been recently revealed as an origin of anxiogenic brain signals, suggesting a target for anxiety treatment. Here, we develop and validate a DBS strategy for modulating anxiety-like symptoms by targeting the LH. We identify a DBS waveform that rapidly inhibits anxiety-implicated LH neural activity and suppresses innate and learned anxiety behaviors in a variety of mouse models. Importantly, we show that the LH DBS displays high temporal and behavioral selectivity: Its affective impact is fast and reversible, with no evidence of side effects such as impaired movement, memory loss, or epileptic seizures. These data suggest that acute hypothalamic DBS could be a useful strategy for managing treatment-resistant anxiety disorders.

deep brain stimulation | anxiety | hypothalamus | orexin | hypocretin

Normal adaptive anxiety behavior ensures survival. In contrast, abnormal persistent anxiety interferes with daily life functioning and may manifest as anxiety disorders. More specifically, fear behavior is an extreme reaction of aversion, characterized by an uncontrollable response to a threatening stimulus. Since in nature, threatening stimuli that induce a fearful state are rarely identical, a fear state is an adaptive neurobiological process to some degree (1). When this normal adaptive process malfunctions, exacerbated fear generalization becomes a marker of psychopathological conditions such as panic or anxiety disorders (2–4).

Anxiety disorders pose one of the biggest challenges to mental health worldwide and represent an economic burden on public health care (5, 6). Anxiety and related disorders are the most common psychiatric disorders worldwide, with a 12-mo prevalence of between 4 and 20% (7, 8). Despite current medications and cognitive therapy, many patients still remain symptomatic. Therefore, there is a need for other modalities as treatment options for anxiety disorders.

In the past century the deep brain stimulation (DBS) method was shown to be an important modality of treatment in various neuropsychiatric disorders such as depression, obsessive-compulsive disorders, movement disorders, obesity, and narcolepsy (9–13). Clinical DBS involves programmable electrical stimulation through an electrode implanted at a specific target in the brain (14). Irrespective of its undoubted promise, there are still many unanswered questions concerning DBS mechanism, actions, specificity, and long-term impact in its application to other pathologies. In addition, there is a lack of consistency in therapeutic DBS effects, which depend on the brain target and disease studied (15, 16).

In this sense, anxiety disorders are a good candidate that would benefit from a more targeted DBS therapy. In this context, the lateral hypothalamus (LH) emerges as a good target region. In particular, the LH neurons producing peptide neurotransmitters orexins/hypocretins (orexin/hypocretin neurons, HONs) have been shown to regulate a wide range of fundamental behavioral and physiological responses such as arousal, as well as the related states of stress and anxiety (17–26). Recently, diverse lines of evidence in humans and animal models suggested that increases in HON activity beyond the level that is needed for normal arousal maintenance may be linked to anxiety-like disorders (27–32).

To this end, we designed a set of experiments to enable us to dissociate states of fear and anxiety-like behaviors, with the aim of testing whether excessive anxiety and fear-related behaviors can be ameliorated by lateral hypothalamic DBS treatment analogous to clinical DBS (9, 10).

Significance

Anxiety disorders are among the most prevalent mental illnesses worldwide. Despite significant advances in their treatment, many patients remain treatment resistant. Thus, new treatment modalities and targets are much needed. Therefore, we developed a deep brain stimulation therapy that targets a recently identified anxiety center in the lateral hypothalamus. We show that this therapy rapidly silences anxiety-implicated neurons and immediately relieves diverse anxiety symptoms in a variety of stressful situations. This therapeutic effect occurs without acute or chronic side effects that are typical of many existing treatments, such as physical sedation or memory deficits. These findings identify a clinically applicable new therapeutic strategy for helping patients to manage treatment-resistant anxiety.

[1]D.P.-R. and D.B. contributed equally to this work.

[2]To whom correspondence may be addressed. Email: daria-peleg@ethz.ch or denis.burdakov@hest.ethz.ch.

Results

Acute Suppression of Anxiety-Implicated Hypothalamic Signals Using DBS. We first sought to examine whether LH DBS can be used in behaving mice to suppress the lateral hypothalamic HON activity implicated in stress and anxiety-like states (22, 24, 25, 27, 33–35). To achieve this, we implanted a DBS electrode in the LH and recorded the activity of surrounding HONs using fiber photometry of the genetically targeted calcium indicator GCaMP6s in behaving mice (Fig. 1 *A* and *B*). We found that application of different frequencies of the classic square monophasic DBS stimulation pattern (36) did not acutely alter HON-GCaMP6s signals (Fig. 1 *C* and *D*: 120 Hz, $P = 0.45$; 2 Hz, $P = 0.32$; one-sample t tests). To rationally design a more effective DBS protocol for accessing HON population activity, we hypothesized that sinusoidal DBS stimulation may be more effective, inspired by recent in vitro patch clamp recordings, indicating that the firing output of isolated HONs can be suppressed by high frequencies of intracellularly injected sinusoidal currents (37). We found that changing the DBS stimulation pattern to the sinusoid waveform (Fig. 1*C*) greatly improved responses of HONs in vivo. Specifically, 120-Hz sinusoid DBS significantly inhibited the HON-GCaMP6s signals (Fig. 1 *C* and *D*: $P < 0.01$; one-sample t test). The 120-Hz sinusoid LH DBS stimulation was significantly more effective at suppressing HON-GCaMP6s activity than 2-Hz sinusoid DBS, or 120 or 2 Hz the square-wave DBS (Fig. 1*D*). Henceforth, we refer to the 120-Hz sinusoid LH DBS as sinusoid high-frequency hypothalamic DBS [shhDBS]). No

evidence of epileptiform brain activity or seizure-like behavior was observed in electroencephalogram (EEG)/electromyogram (EMG) or hippocampal local field potential (LFP) recordings in response to shhDBS (*SI Appendix*, Fig. 1). To investigate whether this way of modulating LH activity alleviates anxiety-like phenotypes, we next sought to establish its efficacy in a variety of mouse models of anxiety disorders.

The Effectiveness of shhDBS in Reducing Innate Anxiety-Like Behaviors. Fear comprises both innate and learned emotional responses that are part of basic survival mechanisms. Unlearned fear, i.e., the innate responses to different stimuli without any previous learning experiences with these stimuli, is used to model some human psychiatric disorders, including anxiety disorders (38, 39). This distinguishes anxiety disorders where there is no known "learned" fear. We tested such innate anxiety and emotionality in an open field (OF) arena and in the elevated plus maze.

In the first phase of the OF test, both mouse groups were not exposed to any stimulation, and baseline locomotor activity was monitored. This locomotor activity was similar between groups, and decreased with time reflecting habituation [Fig. 2 *A* and *B*, two-way repeated measures (RM) ANOVA $F_{(1,8)} = 6.43$, time $P < 0.0001$; group $P = 0.36$]. The time spent in the center of the open field arena is used as a behavioral measure of anxiety (40–42). Time spent in the central zone of the arena did not differ between the groups during the first phase (Fig. 2*C*, t test $P = 0.97$). In the second phase of the OF test, when
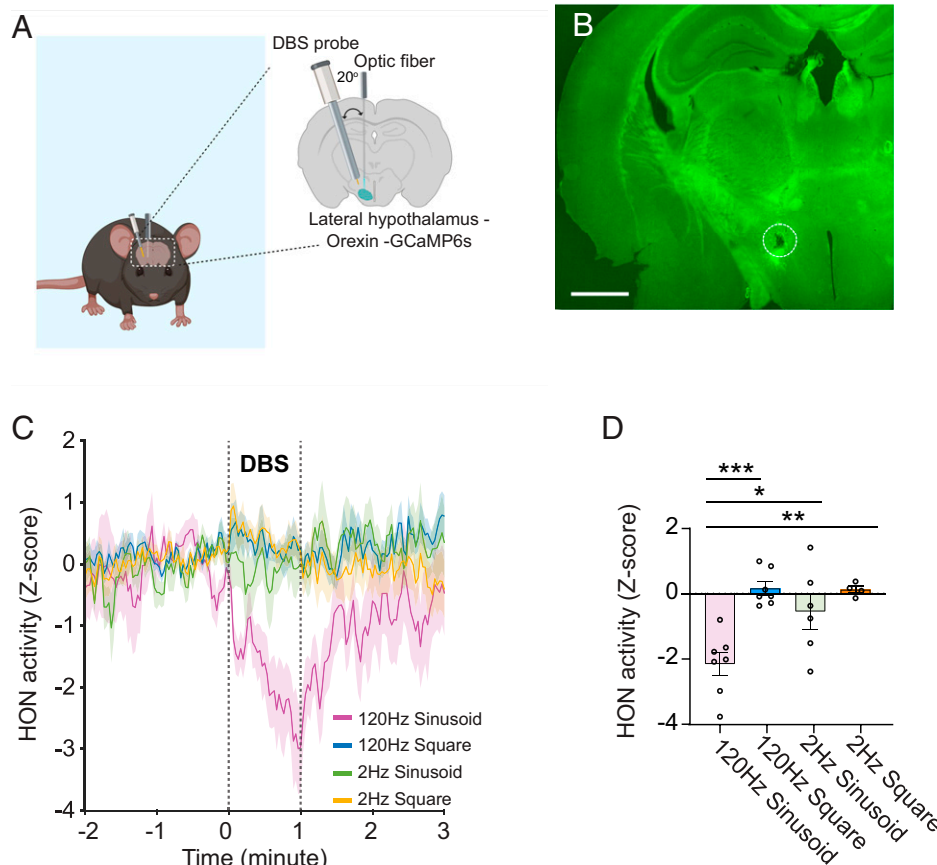
Fig. 1. HON neural activity during different patterns of lateral hypothalamic DBS. (*A*) Targeting schematic for concurrent HON-GCaMP6s fiber photometry and LH DBS. (*B*) Histology image of a representative example of $n = 16$ mice confirming the targeting of the DBS probe tip to the LH (circled). (Scale bar, 1 mm.) (*C*) Orexin-GCaMP6s response to different DBS frequencies and waveforms. (*D*) Quantification of data in *B*, showing DBS-induced changes in HON activity (measured during the 1-min DBS stimulation). One-way RM ANOVA $F_{(3,20)} = 9.252$, $P < 0.001$; Bonferroni posttests: ***$P < 0.001$, **$P < 0.01$, *$P < 0.05$. Data are means $\pm$ SEM of $n = 4$ to 7 mice.

shhDBS stimulation was applied and compared to the control group that received 2-Hz LH DBS, no difference in locomotor activity was detected between the groups (Fig. 2D, two-way RM ANOVA $P = 0.7$). In contrast, shhDBS group significantly increased time spent in the aversive center compared to control mice (Fig. 2E, t test $P < 0.05$).

In the elevated plus maze test, percentage of time spent in the open arms revealed a significant main effect of shhDBS condition (Fig. 2 F and G, t test $P < 0.02$), reflecting an enhanced tendency of the shhDBS condition to spend time in the open arms. In contrast, and consistent with the results obtained in the OF test, general locomotor activity indexed by the total distance moved was comparable between the shhDBS and control conditions (Fig. 2H, t test $P = 0.15$).

The Effects of shhDBS on Conditioned Fear Memory. Acquired (learned) fear triggers characteristic behaviors of escape and avoidance in response to a specific, previously experienced aversive stimulus (i.e., pain or the threat of pain). In this set of experiments, we investigated fear behaviors that become pathological when a response to a potential threat is exaggerated and anxiety becomes abnormal (43–45). To this end, we utilized the fear conditioning paradigm, since it is one of the most translational experimental paradigms for the study of fear-related dimensions of posttraumatic stress disorder (PTSD) (46, 47). In this test, we used a protocol that enables us to identify two independent cue associations, one relating to the unconditioned stimuli (foot shock) linking the context where the initial training acquisition took place, and the other to the neutral cue (tone), which was presented in a novel and neutral context (48, 49).

Because the LH has been proposed to have a central position in adapting to stressful situations (34, 50–52), we were interested in better understanding how shhDBS may influence aversive states and modulate the different dimensions of fear memory. We did not apply shhDBS stimulation during the initial fear learning in order not to interfere with fear memory formation. The development of conditioned freezing was assessed by the amount of freezing across three successive presentations of tone (conditioned stimulus) when it was followed by the shock (unconditioned stimulus) in the conditioning session. Freezing levels increased throughout conditioning [Fig. 3B, two-way RM ANOVA of tone-shock trials $F_{(2,18)} = 49.09$, $P < 0.0001$] and did not differ between the DBS and control conditions [Fig. 3B, two-way RM ANOVA of DBS/control $F_{(1,9)} = 0.17$, $P = 0.69$]. To examine the effect of shhDBS in contextual fear memory, we applied it during subsequent context-evoked fear. There was a general increase in the level of freezing as a function of time in both shhDBS and control groups [Fig. 3C, two-way RM ANOVA of time $F_{(7,63)} = 2.80$, $P < 0.02$], but they did not differ in their context-freezing levels [Fig. 3C, two-way RM ANOVA of DBS/control $F_{(1,9)} = 0.19$, $P = 0.67$], suggesting an intact fear-context memory. In contrast, during extinction of conditioned cued fear, there were profound differences between shhDBS and control animals. While both groups showed a reduction in freezing across an extinction session and across extinction days, overall shhDBS mice exhibited persistently reduced freezing relative to the control group [Fig. 3D, two-way RM ANOVA of DBS/control $F_{(1,9)} = 7.71$, $P < 0.03$; see also *SI Appendix,* Fig.
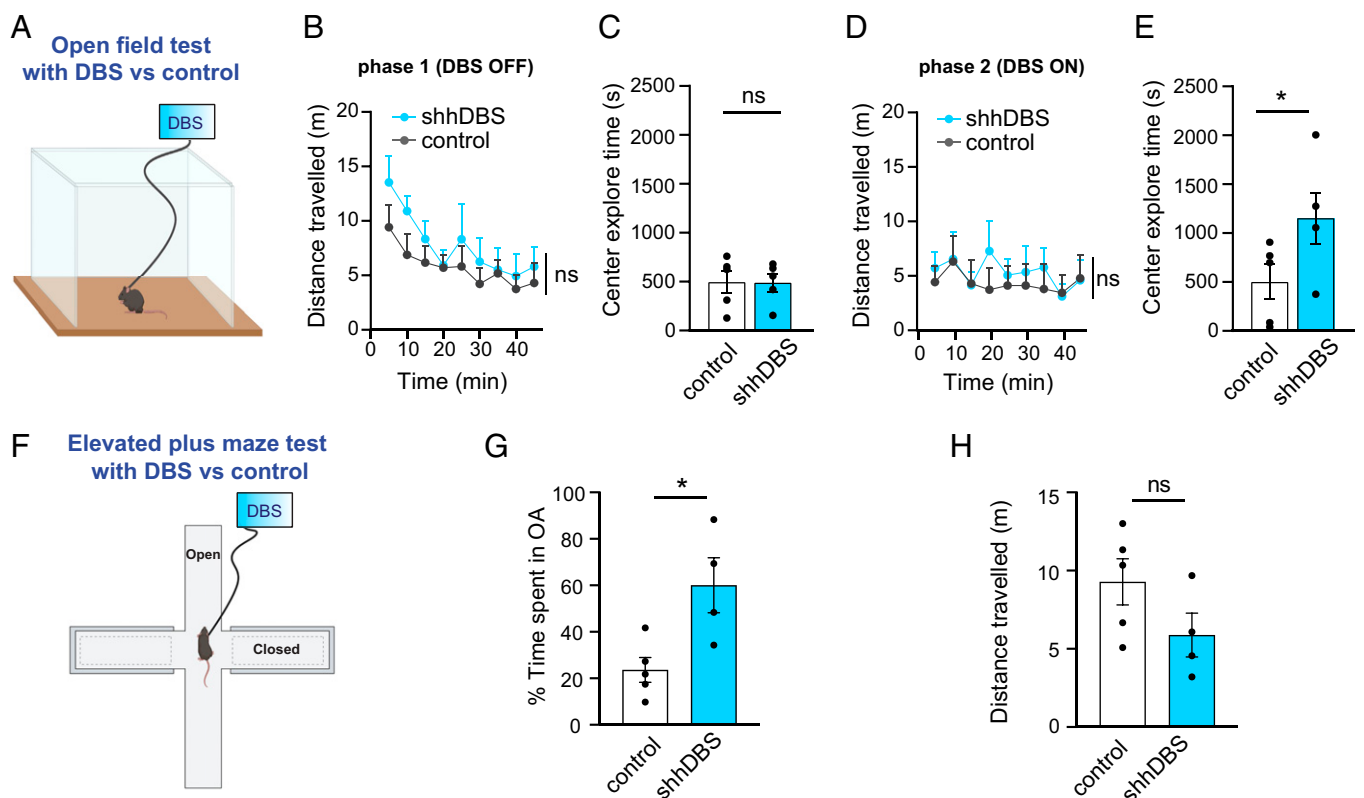
Fig. 2. Effect of lateral hypothalamic DBS on innate anxiety-like behaviors. (A) Schematic of the open field experiment. (B) Distance traveled during pre-DBS habituation (phase 1). (C) Center exploration time during pre-DBS habituation (phase 1). (D) Distance traveled during shhDBS and control conditions (phase 2). (E) Center exploration time during shhDBS and control (phase 2). (F) Schematic of the elevated plus maze DBS experiment. (G) Percentage of time spent in open arms (OA) of the elevated plus maze. (H) Total distance traveled in the elevated plus maze. Data are mean ± SEM of n = DBS/control = 5/5 mice in open field and 4/5 mice in elevated plus maze. In A–E, control is 2-Hz sinusoid DBS, in F–H control is sham. ns, not significant, *P < 0.05 (test details are given in *Results*).

2]. Importantly, when shhDBS was not applied on the fourth extinction training, both experimental groups showed a similar level of freezing behavior (Fig. 3E, two-way RM ANOVA of DBS/control, $P = 0.24$). This indicates that shhDBS has an acute effect when applied and not a long-term persistence after DBS termination in modulating fear behavior.

Emotional Properties of shhDBS. To assess the immediate emotional impact of shhDBS (i.e., rewarding vs. aversive affective state), we asked whether the animal prefers or avoids it using the real-time preference (RTP) test (53). In this test, when an experimental animal entered a counterbalanced shhDBS-designated, contextually indistinct side of the testing arena, shhDBS was constantly applied until the animal exited back into the other side (Fig. 4A). Thus, the mice could freely choose their lateral hypothalamic stimulation pattern and indicate their choice by their presence in shhDBS vs. control side of the testing arena. We found that mice spent significantly more time in the shhDBS side than in the control side (Fig. 4B, t test $P < 0.0001$). This suggests that shhDBS has positive valence. Locomotion velocity did not differ between shhDBS and control sides (Fig. 4C, t test $P = 0.52$; means of velocity control = 10.63 ± 1.47, shhDBS = 9.46 ± 0.98). These data suggest that changes in locomotion cannot explain the increased time spent in the shhDBS side we observed. However, they may indicate that the animals associate the shhDBS side with a positive valence state.

Neuropharmacological Properties of shhDBS. If the emotional impact of shhDBS (Fig. 4B) depends on the suppression of endogenous orexin activity (Fig. 1), then the place preference produced by shhDBS would be expected to be reduced in the presence of orexin receptor antagonism ("floor effect"). When animals were injected with the orexin antagonist SB-334867 (SB) (30 mg/kg intraperitoneally [i.p.]) prior to the RTP test, they no longer displayed a significant preference for the shhDBS side (Fig. 4D, t test $P = 0.09$). Velocity did not differ between shhDBS and control sides after SB injection (Fig. 4E, t test $P = 0.95$; means of velocity after SB injection control = 7.80 ± 2.02, shhDBS = 7.64 ± 1.41). This suggests that the emotional impact of shhDBS may depend on depressing the endogenous orexin tone. Consistent with this possibility, when suppression of HON activity was opposed by optogenetic stimulation (Fig. 4F and *Methods*), the place preference induced by shhDBS (Fig. 4B) was abolished (Fig. 4G, t test $P = 0.19$). Furthermore, we observed significant correlations between the amplitude of shhDBS-induced HON activity depression (measured as in Fig. 1) and the impact of shhDBS on OF center time (Fig. 4H), elevated plus maze percentage open arm time (Fig. 4I), RTP shhDBS preference (Fig. 4J), and the percentage of freezing time on the first day of extinction (Ext1) freezing time (Fig. 4K). In contrast, the percentage of freezing time in the fourth extinction session (Ext4) did not correlate with shhDBS-induced orexin cell activity depression (Fig. 4L). This implies that without shhDBS exposure treatment extinction learning is not facilitated and freezing levels do not differ from the control condition. Furthermore, it suggests that shhDBS modulation is reversible and does not have a long-lasting effect after termination. Overall, these results reveal that shhDBS exerts an emotional and cellular influence that is consistent with its anxiolytic-like effects observed in innate anxiety and learned fear paradigms.

Discussion

DBS has beneficial therapeutic effects in a wide range of neurological disorders. However, despite the progress of DBS in neurology over the last decades, the advancement of DBS in psychiatric disorders has been slower. This is partly due to the heterogenous symptomatology and manifestation of psychiatric disorders and especially in anxiety disorders. Until now there has been little information about DBS efficacy and safety in the treatment of anxiety disorders (54–57). Therefore, application of DBS in animal models of anxiety-like disorders is a fundamental translational approach to a potential targeted therapy. The LH is a promising brain target for this therapy, because it is implicated in cognition and in mood and anxiety disorders, in part through mechanisms involving anxiogenic LH HON activity (27–32, 58–61).

This study demonstrates a DBS stimulation pattern, shhDBS, that silences LH HONs (Fig. 1), rapidly induces positive emotional affect in an orexin-dependent manner (Fig. 4), and acutely decreases anxiety-like symptoms in both innate and learned anxiety settings (Figs. 2 and 3). Importantly, the anxiolytic effects of shhDBS occurred without a general impairment of locomotor activity (Fig. 2 B, D, and H), contextual memory (Fig. 3C), or induction of an epileptiform brain activity (*SI Appendix*, Fig. 1). To the best of our knowledge, no previous evidence suggested that hypothalamic DBS can alleviate symptoms of anxiety disorders, which disable millions of people worldwide and frequently resist existing treatments (62–64).

In models of innate anxiety behaviors, shhDBS acutely resulted in a significant decrease in anxiety-like symptoms without modulating locomotion. Specifically, DBS application rapidly decreased avoidance of innately anxiogenic environments, such as the aversive central zone of the open field and the open arms of the elevated plus maze. In the learned anxiety paradigm, the cued fear conditioning, acute shhDBS (only during the 8 min of tone onset) enhanced fear extinction. The biggest effects of shhDBS were noted during long-term memory timepoints (extinction days 1 to 3, i.e., 48 to 96 h after the initial memory acquisition process). When shhDBS was applied repeatedly over 3 consecutive extinction training days, it reduced fear expression (Fig. 3D). In the fourth extinction session, when shhDBS was not applied, both shhDBS and the groups did not differ in their freezing levels (Fig. 3E). Importantly, this indicates that shhDBS did not eliminate the original fear memory. Thus, shhDBS stimulation does not have a lasting aftereffect on fear extinction, suggesting that shhDBS needs to be applied simultaneously with extinction training in order to facilitate extinction. We can postulate that shhDBS acutely and reversibly induces an emotional state in which extinction from the reexposure to the threat cue is more easily learned and retrieved.

Abnormal fear extinction plays a significant role in many anxiety disorders, specifically in PTSD. Therefore, it is important to understand how fear is diminished and how one stops expressing conditioned responses to a specific stimulus by relearning that the initial stimulus does not impose any danger. Existing treatment interventions of anxiety disorders attempt to inhibit these exaggerated fear responses by facilitating fear extinction (65–67). Our findings imply that shhDBS can acutely decrease fear expression and anxiety symptoms. These properties make shhDBS potentially useful as an augmentation strategy for exposure therapy for PTSD.

Selectivity, controllability, and safety are sought-after qualities in the development of translational therapies. Our findings
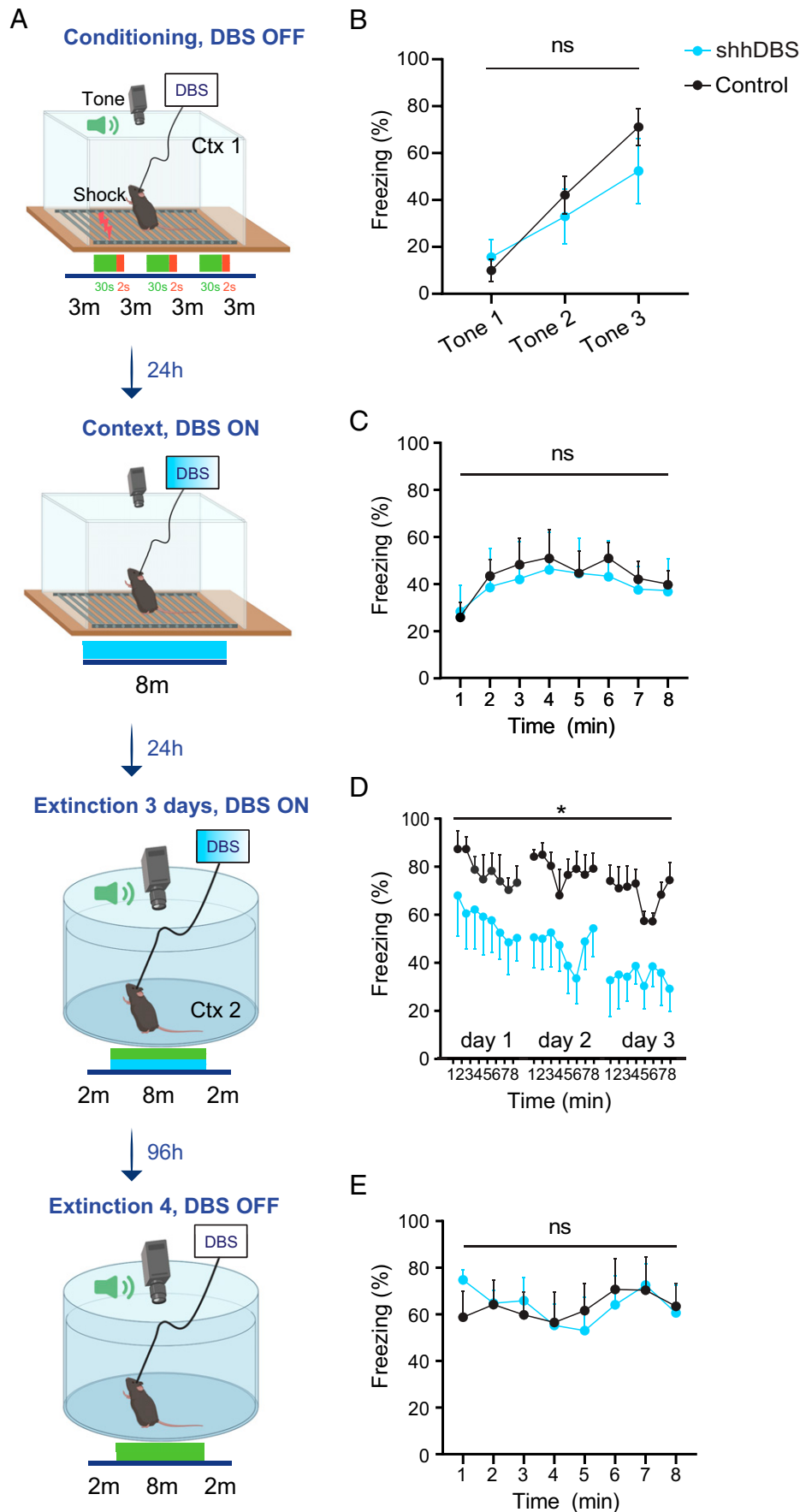
Fig. 3. Effect of lateral hypothalamic DBS on learned fear. (*A*) Schematic of the fear conditioning and extinction experiment showing temporal targeting of shhDBS. Ctx 1, ctx 2 = contexts 1 and 2. Green, tone; red, footshock; blue, shhDBS. (*B*) Freezing during the 30-s tone trials in conditioning phase (DBS not applied), demonstrating normal fear learning. (*C*) Freezing during the 8-min context phase (DBS applied in shhDBS animals). (*D*) Freezing during 8-min tone in the three extinction sessions (DBS applied in shhDBS animals). (*E*) Freezing during 8-min tone in the fourth extinction session (DBS not applied). Data are means ± SEM of *n* = 5 shhDBS and *n* = 6 control (sham) mice. ns, not significant, *P < 0.05 (test details are given in *Results*).
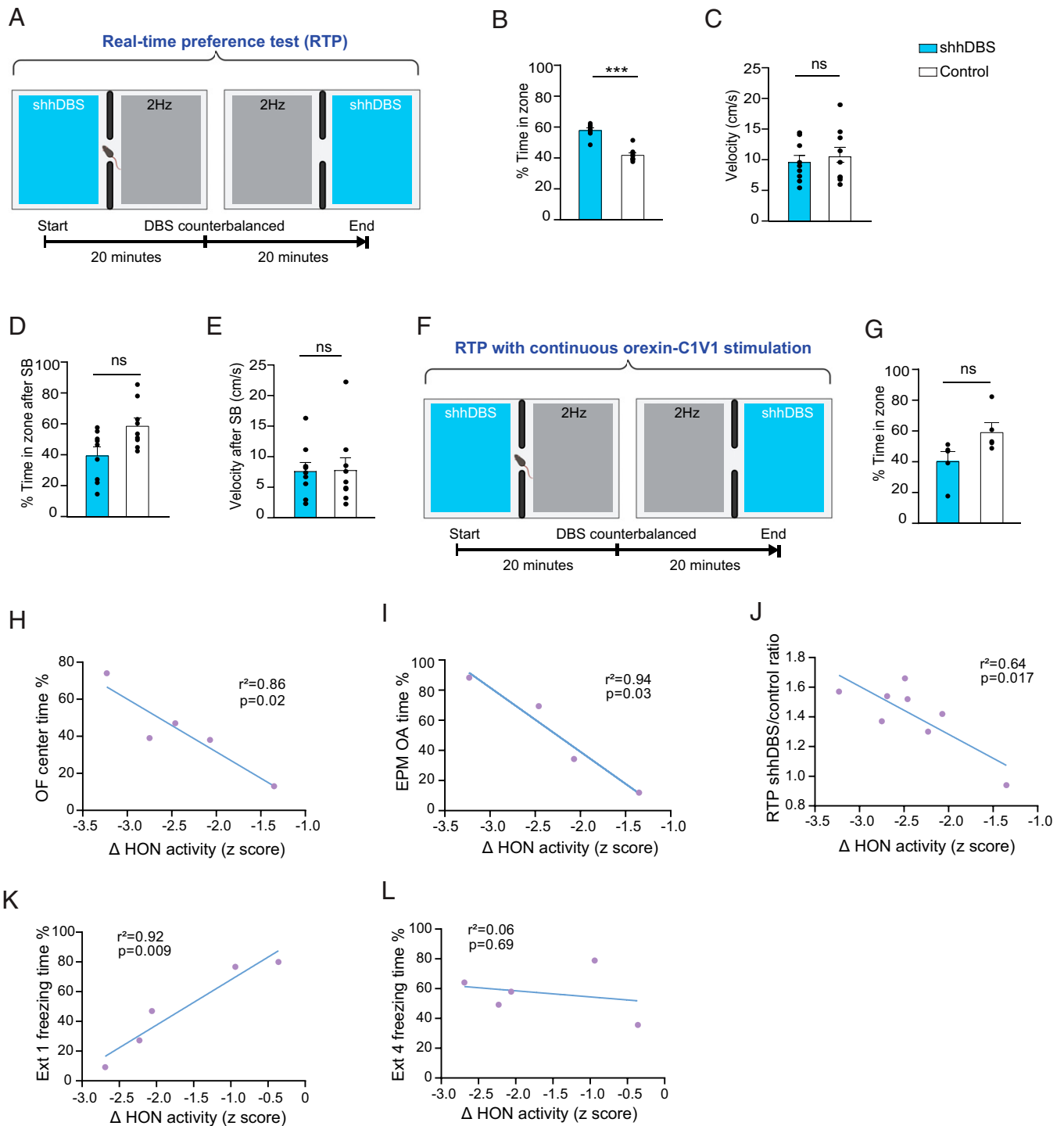
Fig. 4. Emotional and neuropharmacological features of lateral hypothalamic DBS. (*A*) Schematic of the RTP test. (*B*) Occupancy of shhDBS and control zones. (*C*) Locomotion in shhDBS and control zones. (*D*) Occupancy of shhDBS and control zones after orexin antagonist SB-334867 (SB). (*E*) Locomotion velocity in shhDBS and control zones after orexin antagonist SB. (*F*) Schematic of the RTP test performed in the presence of optogenetic stimulation of HONs (orexin-C1V1 stimulation). (*G*) Occupancy of shhDBS and control zones during the optogenetic HON stimulation. (*H*) Correlation between shhDBS-induced HON-GCaMP6s inhibition and shhDBS effects on open field (OF) center occupancy. (*I*) Correlation between shhDBS-induced HON-GCaMP6s inhibition and shhDBS effects on elevated plus maze (EPM) OA occupancy. (*J*) Correlation between shhDBS-induced HON-GCaMP6s inhibition and shhDBS-induced place preference (ratio of time spent in shhDBS and control zones) in the RTP test. (*K*) Correlation between shhDBS-induced HON-GCaMP6s inhibition and shhDBS effects on cued fear expression during extinction day 1 (Ext1). (*L*) Control data, confirming lack of correlation between shhDBS-induced HON-GCaMP6s inhibition and post-shhDBS effects on cued fear expression during Ext4. (Fig. 3*A*). (*B*–*E*) Data are mean ± SEM of *n* = 9 mice. (*G*) Data are mean ± SEM of *n* = 5 mice; ns, not significant, ***$P < 0.001$. (*H*–*L*) Each point represents one mouse, r^2 and *P* values are from Pearson correlation tests. Control is 2-Hz sinusoid DBS.

demonstrate that shhDBS leads to reduction in anxiety-like behaviors only during the stimulation, and that these effects are readily reversible after stimulation stops, without detectable long-term motor impairment or memory loss. This suggests a good temporal selectivity and controllability of shhDBS effects, possibly related to its effects on anxiety rather than on plasticity/memory as discussed above. In addition, body temperature and corticosterone levels were not altered by shhDBS (*SI*

Appendix, Fig. 3). The selective targeting of anxiety without observable impact on locomotion implies little effect of shhDBS on general motivation to move, as well as on motor control. This is an important feature of acute shhDBS treatment, because severe reduction in LH activity (for example, caused by complete deletion of HONs or by LH electrolytic lesions) has been linked to profound loss of motivation and motor activity (68, 69). While we found that shhDBS reduced an aspect of LH activity, consistent with its anxiolytic properties, this reduction was presumably not so severe as to cause the general psychomotor impairment reported for LH lesions. It is also likely that, in addition to LH HONs, shhDBS modulates other neural systems not studied here. In theory, such modulation upstream or downstream of HONs could contribute to both HON modulation and to suppression of side effects. Finally, our anxiolytic shhDBS application was not associated with an epileptiform brain activity, a key concern in DBS applications (70, 71). Of note, the latter finding does not imply that shhDBS has no effect on physiological brain oscillations; whether it alters oscillations in cognitively important areas such as the hippocampus (72) and the relation of such alterations to therapeutic effects are important subjects for future investigation. Overall, shhDBS thus has key desirable properties for potential future translational applications.

In conclusion, our data suggest that brief hypothalamic DBS could be a useful strategy to augment treatment for anxiety- and trauma-related disorders to help to combat symptoms and prevent relapse. Targeting of the hypothalamus with DBS is feasible in human patients (73), in principle allowing future assessments of whether certain hypothalamic DBS stimulation patterns could be effective in human anxiety disorders. In contrast to current PTSD treatment options, such as cognitive-behavioral therapy and antidepressant medications, DBS has the potential to specifically modulate the activity of a brain region that was previously not therapeutically targeted in this disorder. Such targeted therapy could lead to better therapeutic efficacy and lower side effects, and it provide a treatment option for PTSD patients that are nonresponders to current therapy.

Methods

Subjects. C57BL/6 mice (Charles River Laboratories) were kept on a standard chow, water ad libitum, and on a reversed 12-h/12-h dark/light cycle. All experiments were performed during the dark phase. Adult males (at least 8 wk old) were used for experiments (total 16 DBS and 15 control mice). Animal experiments followed United Kingdom Home Office regulations or the Swiss Federal Food Safety and Veterinary Office Welfare Ordinance (TSchV 455.1, approved by the Zürich Cantonal Veterinary Office).

Surgical Procedures. Mice were anesthetized with isoflurane and then placed in a stereotaxic frame (Kopf Instruments). A single dose of Metacam (10 μL/g) was injected subcutaneously before surgery. To express a genetically targeted activity indicator in HONs, a previously validated and characterized AAV1-hORX.GCaMP6s vector (74, 75) was injected into the LH. A Hamilton syringe was used to inject 150 to 250 nL of AAV1-hORX.GCaMP6s over the LH (bregma, −1.35 mm; midline, ±0.90 mm; depth, 5.40 mm) at a rate of 50 nL/min. A fiberoptic implant for measuring GCaMP6s fluorescence (Thorlabs) was then stereotaxically implanted with the fiber tip above the lateral hypothalamus at a depth of 5.0 mm. For experiments with a DBS electrode, a bipolar concentric stimulation electrode (P1 Technologies, custom 1-mm contact separation) was implanted unilaterally on the same LH side as the fiberoptic at bregma, −1.35 mm; midline, ±2.70 mm; depth, 5.10 to 5.20 mm, with a 20-degree angle. For the EEG and EMG surgery, a three-channel EEG headmount (Pinnacle Technology) with four stainless steel screws that acted as cortical surface electrodes were installed into the skull. Anterior screws were 1 mm anterior to bregma and 1 mm lateral from the midline on each side. Posterior screws were 4.5 mm posterior to bregma and 2 mm lateral from the midline. The left anterior screw served as the ground connection. A pair of wires were embedded into the bilateral neck muscle to monitor EMG signals. All the implanted probes and headmounts were fixed to the skull with dental cement (Superbond universal kit, Hentschel-Dental).

Experimental DBS Protocol. A bipolar cable (P1 Technologies) was connected from an amplifier (Heka EPC-10) to the DBS electrode to deliver an electric stimulus. Stimulation was programmed by Patchmaster software (Heka Elektronik) and operated through the amplifier. Continuous periodic oscillation waveforms were delivered at frequencies of either 2 or 120 Hz for the sinusoidal waveforms. The peak-to-peak voltage amplitude was 2.0 to 4.0 V, which was tested in an escalating fashion for each mouse to find a consistent HON signal inhibition without seizure provocation or other behavioral abnormalities. For the square waveforms, we utilized monophasic pulses of similar amplitude, with a pulse width of 10 to 100 μs based on previous DBS literature (36, 76, 77). The stimulation duration was 1 min for the fiber photometry experiment. For other behavioral experiments, the duration varied as described in each section of *Methods*. During all measurements, both shhDBS and control animals were implanted with DBS electrodes and tethered to the stimulator, but only the shhDBS group was stimulated using shhDBS. The control group was either not stimulated or stimulated at a 2-Hz sinusoid waveform; no differences were observed between these two control conditions and they were used interchangeably in the study, as indicated in the figure legends.

Fiber Photometry, EEG–EMG, and LFP Recordings. Lateral hypothalamic fiber photometry was performed using the Doric fiber photometry system, in interleaved mode providing alternating (10 Hz) 405- and 465-nm excitation light pulses via two light-emitting diodes (LEDs), similar to our previous work (78, 79). The LED power for 405 and 465 nm was ∼100 μW at the fiber tip. Data were acquired using the Spike2 software (Cambridge Electronic Design). To correct any linear signal bleaching, raw GCaMP6s fluorescence traces produced by 405- and 465-nm excitation were first detrended using a linear fit through the median first and last 50 s of a 7-min time window centered on the period of DBS stimulation. The traces were then z score normalized using median and SD of the trace baseline during the 60 s prior to stimulation (i.e., for each peristimulation time epoch, the baseline median was subtracted from each point, and the result was then divided by the baseline SD). Finally, to produce the HON activity plots in Fig. 1, for each recording the processed (as above) 405-excitation trace was subtracted from the 465-excitation trace; this procedure corrects for any movement artifacts because the 405 excitation is an isosbestic point of GCaMP, which reports movement artifacts but not neural Ca^{2+} activity (80). In Fig. 4 *H–L*, Δ HON activity was quantified as the difference between pre-shhDBS HON-GCaMP6s activity and minimum HON-GCaMP6s activity (i.e., largest response amplitude) during the first minute of shhDBS application. For the EEG/EMG recordings (*SI Appendix,* Fig. 1), EEG and EMG data were acquired at a 1-kHz sample rate by a standard acquisition system with a commercial preamplifier (Pinnacle Technology; 10× gain) and recorded by the Spike2 software to synchronize the time stamp with the photometry data.

For the LFP recording (*SI Appendix,* Fig. 1*C*), mice were anesthetized with an i.p. injection of ketamine (100 mg/kg) and xylazine (10 mg/kg) and fixed in a stereotaxic frame. The skull was exposed, burr holes were created, and a recording electrode made of silver wire (Harvard Apparatus, AG10W) was placed in the CA1 region at the following coordinates: bregma, −2.06 mm; midline, 1.30 mm; depth, 1.15 to 1.25 mm. Two screws were placed over the bilateral cerebellum to serve as ground and reference electrodes. The electrodes were connected to an EEG headstage (Pinnacle Technology, 8235: 6-pin headmount), and LFPs were recorded by the Spike2 software after resting for 15 min for stabilization.

EEG/EMG and LFP data were analyzed in MATLAB. EEG and LFP signals were filtered with a low-pass filter at 100 Hz to remove stimulation artifacts, and a second order 50-Hz notch filter to remove line noise. In the *Bottom Left* plot of *SI Appendix,* Fig. 1*C*, the raw LFP trace was first time stamped to define 5 s before, during stimulation, and after stimulation. Next, the Welch method was used to compute the mean power spectral density estimate.

Optogenetics. Optogenetic stimulation of HONs (Fig. 4 *F* and *G*) was performed as in ref. 75. In brief, HON-targeting viral vector containing the excitatory opsin C1V1 was bilaterally injected into the LH (AAV1-hORX.C1V1(t/s).mCherry viral vector, which targets HONs with >96% specificity, as verified by histological analysis of the LH (75). After 2 wk of expression, bilateral optogenetic stimulation of HON-C1V1 cells was performed via LH fiberoptic implants using 532-nm green lasers (Laserglow) (5-ms flash duration, 10-Hz flash frequency, and ~10 mW at fiber tip), as in ref. 75. For optogenetic epileptic seizure induction (*SI Appendix*, Fig. 1*B*), mice were injected in the left dorsal hippocampus (bregma, −2.06 mm; left, 1.30 mm; depth, 1.25 mm) with AAV9-CaMKIIa.C1V1(t/t).TS.EYFP (Addgene) for induction of the seizure as previously described (81). To induce the seizure, a 532-nm laser at ~10 mW at the optic fiber tip was applied to the dorsal hippocampus for 10 s.

Body Temperature and Corticosterone Measurements. For corticosterone measurements, we employed a noninvasive technique to monitor stress hormone metabolites in fecal samples (82, 83). Fecal sample collections were performed during the dark phase of the light–dark cycle and conducted under dimmed light conditions to avoid disturbing the animals' natural activity rhythm. Samples were collected during 8 min of shhDBS application. Fecal corticosterone levels were analyzed in duplicate using DRG-Diagnostics corticosterone competitive enzyme-linked immunosorbent assay (ELISA) (EIA-4164; DRG Instruments GmbH), in accordance with the manufacturer's instructions. Body temperature was measured during shhDBS application using an infrared thermometer (Reichelt Elektronik UT 305H, Uni-Trend Technology).

Spontaneous Locomotor Activity and Anxiety-Like Behaviors in the Open Field. The apparatus consisted of four identical open-field arenas (40 cm × 40 cm × 35 cm high). The arenas were located in a testing room under dim diffused lighting. A digital camera was mounted directly above the arenas, capturing images from all four arenas at a rate of 5 Hz. The images were then transmitted to a personal computer (PC) running the Ethovision XT tracking system (Noldus Technology), and spontaneous locomotor activity and time spent in the center portion of the arena were assessed in two different testing phases. Activity was indexed by the distance traveled in centimeters in the entire arena, expressed as a function of nine successive 5-min bins and time spent in seconds in the central zone of the arena. In the first phase, the first 45 min animals habituated to the arena and in the second phase, either 2-Hz sinusoid DBS or 120-Hz sinusoid DBS was applied for another 45 min.

Elevated Plus Maze. The elevated plus maze consisted of two exposed and two enclosed arms joined to a central square platform. Its construction has previously been described in detail (84, 85). The maze was located in a dimly lit experimental room. A digital camera was mounted above the maze, and images captured at a rate of 5 Hz were transmitted to a PC running the Ethovision XT tracking system (Noldus Technology). The mouse was gently placed in the central square facing one of the open arms. It was then allowed to move undisturbed for 5 min. Two measures were taken: percentage of time spent in the open arms (time in the open arms/time in all arms × 100%) and the total distance traveled in the entire maze as a measure of general locomotor activity. The shhDBS started when the animal was placed on the maze and lasted for 5 min (the total length of the test).

Pavlovian Conditioned Freezing. The apparatus consisted of two distinct sets of two test chambers, providing two different contexts. The first set of chambers (used for initial fear learning on day 1 and context freezing on day 2) comprised two operant chambers (Model E10-10, Coulbourn Instruments), each installed in a ventilated, sound-insulated chest. Each testing box was equipped with a grid floor made of stainless steel rods. A scrambled electric shock 2 s in duration and 0.3 mA in intensity was delivered (model E13-14, Coulbourn Instruments). The mouse was confined to a rectangular Plexiglas enclosure (17.5 cm × 13 cm).

The second set of chambers (used for fear extinction on days 3 to 5 and day 8) comprised two Plexiglas cylindrical enclosures (19 cm in diameter) fixed on a white plastic floor, with each located in a ventilated, sound-insulated wooden box. Tone (2.9 kHz, 90 dB) was delivered through intrachamber speakers. Sessions were recorded with a built-in infrared (IR) camera (30 fps), and an automated video tracing system (Noldus EthoVision XT) was used to analyze freezing behavior. The protocol consisted of four distinct phases: Phase 1 was conditioning (Fig. 3*B*). All mice were given three conditioning trials. Each trial consisted of a 30-s tone stimulus followed immediately by a 2-s, 0.3-mA foot shock. The first trial was administered 3 min after the mice were placed into the chambers. Successive trials were administered every 3 min. The conditioning session concluded with a final 3-min interval. Phase 2 was a test of conditioned context freezing (DBS was applied; Fig. 3*C*). The mice were returned to the same context and placed in the test chamber for a period of 8 min when DBS was applied immediately when the test started and lasted 8 min. Phase 3 was a test of conditioned tone freezing. On testing days 3 to 5, the conditioned-stimulus (CS) freezing to the tone stimulus was assessed in a novel context. The tone stimulus was administered 2 min after the mice were placed into the test chamber and then the tone remained continuously for a period of 8 min and concluded with a final 2 min of no stimulus. DBS was applied across the 3 extinction days (Fig. 3*D*) simultaneously during the onset of the tone for 8 min. Phase 4 was a test of conditioned tone freezing in the novel box the same as for Fig. 3*C* but without DBS exposure (Fig. 3*E*).

RTP Test. The apparatus consisted of a rectangular arena (50 × 25 × 25 cm) with two identical sides separated by an open door. One side was paired with shhDBS and the other with non-shhDBS (control stimulation, 2-Hz sinusoid DBS). The mouse was allowed to freely explore the apparatus for two sessions, each lasting 20 min. In each session, percentage of time in shhDBS and non-shhDBS sides was calculated by dividing the time spent in the side by the total time of the test.

Histology. Mice were sedated with an i.p injection of pentobarbital and transcardially perfused with 4% paraformaldehyde . The brain implants were carefully removed, and brains were postfixed for 24h and transferred to phosphate buffered saline for storage. Coronal brain slices were sectioned at 50μm using a cryostat. Micrographs were acquired by Nikon Eclipse Ti2 and edited in ImageJ.

Data Analysis. Data were analyzed using Prism 9 (GraphPad Software Inc.) and MATLAB 2019b (Mathworks). Before parametric tests, data were assessed for normality with a D'Agostino–Pearson omnibus test or Kolmogorov–Smirnov test for small sample sizes. To compare interactions within normally distributed data with repeated measurements, RM ANOVA was used, with multiple comparison tests where appropriate. Data are presented as mean ± SEM in the result and figures. *P* values <0.05 were considered statistically significant.

Data Availability. All study data are included in the article and/or supporting information.

Author affiliations: ªSection of Epilepsy, Department of Neurology, Chang Gung Memorial Hospital at Linkou Medical Center and Chang Gung University College of Medicine, 333 Taoyuan, Taiwan; ᵇDepartment of Health Sciences and Technology, Institute for Neuroscience, ETH Zürich, 8603 Schwerzenbach, Switzerland; ᶜDepartment of Health Sciences and Technology, Institute of Food, Nutrition, and Health, ETH Zürich, 8603 Schwerzenbach, Switzerland; and ᵈNeuroscience Center Zürich, 8057 Zürich, Switzerland

1. A. Asok, E. R. Kandel, J. B. Rayman, The neurobiology of fear generalization. *Front. Behav. Neurosci.* **12**, 329 (2019).
2. S. Lissek et al., Overgeneralization of conditioned fear as a pathogenic marker of panic disorder. *Am. J. Psychiatry* **167**, 47–55 (2010).
3. S. Lissek et al., Generalized anxiety disorder is associated with overgeneralization of classically conditioned fear. *Biol. Psychiatry* **75**, 909–915 (2014).
4. J. E. Dunsmoor, R. Paz, Fear generalization and anxiety: Behavioral and neural mechanisms. *Biol. Psychiatry* **78**, 336–343 (2015).

5. D. J. Nutt et al., Consensus statement on the benefit to the community of ESEMeD (European Study of the Epidemiology of Mental Disorders) survey data on depression and anxiety. *J. Clin. Psychiatry* **68** (suppl. 2), 42–48 (2007).
6. K. R. Merikangas et al.; Zurich Cohort Study, Longitudinal trajectories of depression and anxiety in a prospective community study: The Zurich Cohort Study. *Arch. Gen. Psychiatry* **60**, 993–1000 (2003).
7. R. Mago, J. P. Gomez, N. Gupta, E. J. Kunhel, Anxiety in medically ill patients. *Curr. Psychiatry Rep.* **8**, 228–233 (2006).

8. J. K. Hirsch, K. L. Walker, E. C. Chang, J. M. Lyness, Illness burden and symptoms of anxiety in older adults: Optimism and pessimism as moderators. *Int. Psychogeriatr.* **24**, 1614–1621 (2012).

9. K. H. Lee, P. S. Duffy, C. D. Blaha, "Overview of the history and application of deep brain stimulation" in *Deep Brain Stimulation* (Pan Stanford Publishing Pte. Ltd., 2016), pp. 3–24.

10. S. Miocinovic, S. Somayajula, S. Chitnis, J. L. Vitek, History, applications, and mechanisms of deep brain stimulation. *JAMA Neurol.* **70**, 163–171 (2013).

11. A. L. Benabid, P. Pollak, A. Louveau, S. Henry, J. de Rougemont, Combined (thalamotomy and stimulation) stereotactic surgery of the VIM thalamic nucleus for bilateral Parkinson disease. *Appl. Neurophysiol.* **50**, 344–346 (1987).

12. D. J. Lee, C. S. Lozano, R. F. Dallapiazza, A. M. Lozano, Current and future directions of deep brain stimulation for neurological and psychiatric disorders. *J. Neurosurg.* **131**, 333–342 (2019).

13. A. A. Rogers *et al.*, Deep brain stimulation of hypothalamus for narcolepsy-cataplexy in mice. *Brain Stimul.* **13**, 1305–1316 (2020).

14. A. M. Lozano *et al.*, Deep brain stimulation: Current challenges and future directions. *Nat. Rev. Neurol.* **15**, 148–160 (2019).

15. K. H. Lee *et al.*, Evolution of Deep Brain Stimulation: Human electrometer and smart devices supporting the next generation of therapy. *Neuromodulation* **12**, 85–103 (2009).

16. R. S. Shah *et al.*, Deep brain stimulation: Technology at the cutting edge. *J. Clin. Neurol.* **6**, 167–182 (2010).

17. L. de Lecea *et al.*, The hypocretins: Hypothalamus-specific peptides with neuroexcitatory activity. *Proc. Natl. Acad. Sci. U.S.A.* **95**, 322–327 (1998).

18. T. Sakurai, The role of orexin in motivated behaviours. *Nat. Rev. Neurosci.* **15**, 719–731 (2014).

19. S. M. Tyree, J. C. Borniger, L. de Lecea, Hypocretin as a hub for arousal and motivation. *Front. Neurol.* **9**, 413 (2018).

20. T. Sakurai *et al.*, Orexins and orexin receptors: A family of hypothalamic neuropeptides and G protein-coupled receptors that regulate feeding behavior. *Cell* **92**, 573–585 (1998).

21. B. Boutrel *et al.*, Role for hypocretin in mediating stress-induced reinstatement of cocaine-seeking behavior. *Proc. Natl. Acad. Sci. U.S.A.* **102**, 19168–19173 (2005).

22. P. Bonnavion, A. C. Jackson, M. E. Carter, L. de Lecea, Antagonistic interplay between hypocretin and leptin in the lateral hypothalamus regulates stress responses. *Nat. Commun.* **6**, 1–14 (2015).

23. T. Kuwaki, "Orexin links emotional stress to autonomic functions" in *Autonomic Neuroscience: Basic and Clinical* (Elsevier, 2011), pp. 20–27.

24. M. Suzuki, C. T. Beuckmann, K. Shikata, H. Ogura, T. Sawai, Orexin-A (hypocretin-1) is possibly involved in generation of anxiety-like behavior. *Brain Res.* **1044**, 116–121 (2005).

25. W. Heydendael, A. Sengupta, S. Beck, S. Bhatnagar, Optogenetic examination identifies a context-specific role for orexins/hypocretins in anxiety-related behavior. *Physiol. Behav.* **130**, 182–190 (2014).

26. D. W. Pfaff, E. M. Martin, A. C. Ribeiro, Relations between mechanisms of CNS arousal and mechanisms of stress. *Stress* **10**, 316–325 (2007).

27. P. L. Johnson *et al.*, A key role for orexin in panic anxiety. *Nat. Med.* **16**, 111–115 (2010).

28. P. L. Johnson, A. Molosh, S. D. Fitz, W. A. Truitt, A. Shekhar, Orexin, stress, and anxiety/panic states. *Prog. Brain Res.* **198**, 133–161 (2012).

29. M. H. James, E. J. Campbell, C. V. Dayas, Role of the orexin/hypocretin system in stress-related psychiatric disorders. *Curr. Top. Behav. Neurosci.* **33**, 197–219 (2017).

30. D. Sargin, The role of the orexin system in stress response. *Neuropharmacology* **154**, 68–78 (2019).

31. O. F. Akça, N. Uzun, İ. Kılınç, Orexin A in adolescents with anxiety disorders. *Int. J. Psychiatry Clin. Pract.* **24**, 127–134 (2020).

32. Á. Flores *et al.*, The hypocretin/orexin system mediates the extinction of fear memories. *Neuropsychopharmacology* **39**, 2732–2741 (2014).

33. C. Blomeley, C. Garau, D. Burdakov, Accumbal D2 cells orchestrate innate risk-avoidance according to orexin signals. *Nat. Neurosci.* **21**, 29–32 (2018).

34. R. Winsky-Sommerer *et al.*, Interaction between the corticotropin-releasing factor system and hypocretins (orexins): A novel circuit mediating stress response. *J. Neurosci.* **24**, 11439–11448 (2004).

35. E. A. Lungwitz *et al.*, Orexin-A induces anxiety-like behavior through interactions with glutamatergic receptors in the bed nucleus of the stria terminalis of rats. *Physiol. Behav.* **107**, 726–732 (2012).

36. Z. Wang, Q. Wang, Eliminating absence seizures through the deep brain stimulation to thalamus reticular nucleus. *Front. Comput. Neurosci.* **11**, 22 (2017).

37. C. Kosse, D. Burdakov, Fast and slow oscillations recruit molecularly-distinct subnetworks of lateral hypothalamic neurons *in situ*. *eNeuro* **5**, 1–9 (2018).

38. N. M. Boulis, M. Davis, Footshock-induced sensitization of electrically elicited startle reflexes. *Behav. Neurosci.* **103**, 504–508 (1989).

39. D. L. Walker, M. Davis, Double dissociation between the involvement of the bed nucleus of the stria terminalis and the central nucleus of the amygdala in startle increases produced by conditioned versus unconditioned fear. *J. Neurosci.* **17**, 9375–9383 (1997).

40. L. Prut, C. Belzung, The open field as a paradigm to measure the effects of drugs on anxiety-like behaviors: A review. *Eur. J. Pharmacol.* **463**, 3–33 (2003).

41. A. Ramos, E. Pereira, G. C. Martins, T. D. Wehrmeister, G. S. Izídio, Integrating the open field, elevated plus maze and light/dark box to assess different types of emotional behaviors in one single trial. *Behav. Brain Res.* **193**, 277–288 (2008).

42. T. Steimer, Animal models of anxiety disorders in rats and mice: Some conceptual issues. *Dialogues Clin. Neurosci.* **13**, 495–506 (2011).

43. A. Ohman, S. Mineka, Fears, phobias, and preparedness: Toward an evolved module of fear and fear learning. *Psychol. Rev.* **108**, 483–522 (2001).

44. R. Nesse, Emotional disorders in evolutionary perspective. *Br. J. Med. Psychol.*, **71**, 397–415 (1998).

45. S. L. Lima, Nonlethal effects in the ecology of predator-prey interactions: What are the ecological effects of anti-predator decision-making? *Bioscience* **48**, 25–34 (1998).

46. S. Maren, G. J. Quirk, Neuronal signalling of fear memory. *Nat. Rev. Neurosci.* **5**, 844–852 (2004).

47. S. Maren, Pavlovian fear conditioning as a behavioral assay for hippocampus and amygdala function: Cautions and caveats. *Eur. J. Neurosci.* **28**, 1661–1666 (2008).

48. J. J. Kim, M. S. Fanselow, Modality-specific retrograde amnesia of fear. *Science* **256**, 675–677 (1992).

49. R. G. Phillips, J. E. LeDoux, Differential contribution of amygdala and hippocampus to cued and contextual fear conditioning. *Behav. Neurosci.* **106**, 274–285 (1992).

50. T. Kuwaki, Orexin links emotional stress to autonomic functions. *Auton. Neurosci.* **161**, 20–27 (2011).

51. T. Kuwaki, W. Zhang, Orexin neurons and emotional stress. *Vitam. Horm.* **89**, 135–158 (2012).

52. W. J. Giardino, L. de Lecea, Hypocretin (orexin) neuromodulation of stress and reward pathways. *Curr. Opin. Neurobiol.* **29**, 103–108 (2014).

53. A. M. Stamatakis, G. D. Stuber, Activation of lateral habenula inputs to the ventral midbrain promotes behavioral avoidance. *Nat. Neurosci.* **15**, 1105–1107 (2012).

54. A. van Dijk *et al.*, Deep brain stimulation affects conditioned and unconditioned anxiety in different brain areas. *Transl. Psychiatry* **3**, e289 (2013).

55. J. Rodriguez-Romaguera, F. H. Do Monte, G. J. Quirk, Deep brain stimulation of the ventral striatum enhances extinction of conditioned fear. *Proc. Natl. Acad. Sci. U.S.A.* **109**, 8764–8769 (2012).

56. J. P. Langevin *et al.*, Deep brain stimulation of the basolateral amygdala for treatment-refractory posttraumatic stress disorder. *Biol. Psychiatry* **79**, e82–e84 (2016).

57. J. M. Baas, No impact of deep brain stimulation on fear-potentiated startle in obsessive-compulsive disorder. *Front. Behav. Neurosci.* **8**, 305 (2014).

58. M. J. Sharpe, H. M. Batchelor, L. E. Mueller, M. P. H. Gardner, G. Schoenbaum, Past experience shapes the neural circuits recruited for future learning. *Nat. Neurosci.* **24**, 391–400 (2021).

59. J. C. Jimenez *et al.*, Anxiety cells in a hippocampal-hypothalamic circuit. *Neuron* **97**, 670–683 (2018).

60. C. Garau, C. Blomeley, D. Burdakov, Orexin neurons and inhibitory Agrp→orexin circuits guide spatial exploration in mice. *J. Physiol.* **598**, 4371–4383 (2020).

61. W. J. Giardino *et al.*, Parallel circuits from the bed nuclei of stria terminalis to the lateral hypothalamus drive opposing emotional states. *Nat. Neurosci.* **21**, 1084–1095 (2018).

62. R. C. Kessler *et al.*, Lifetime prevalence and age-of-onset distributions of DSM-IV disorders in the National Comorbidity Survey Replication. *Arch. Gen. Psychiatry* **62**, 593–602 (2005).

63. K. M. Myers, M. Davis, Mechanisms of fear extinction. *Mol. Psychiatry* **12**, 120–150 (2007).

64. D. J. Stein, K. M. Scott, P. de Jonge, R. C. Kessler, Epidemiology of anxiety disorders: From surveys to nosology and back. *Dialogues Clin. Neurosci.* **19**, 127–136 (2017).

65. M. A. Lynch, Long-term potentiation and memory. *Physiol. Rev.* **84**, 87–136 (2004).

66. R. Richardson, L. Ledgerwood, J. Cranney, Facilitation of fear extinction by D-cycloserine: Theoretical and clinical implications. *Learn. Mem.* **11**, 510–516 (2004).

67. L. Ledgerwood, R. Richardson, J. Cranney, Effects of D-cycloserine on extinction of conditioned freezing. *Behav. Neurosci.* **117**, 341–349 (2003).

68. D. R. Levitt, P. Teitelbaum, Somnolence, akinesia, and sensory activation of motivated behavior in the lateral hypothalamic syndrome. *Proc. Natl. Acad. Sci. U.S.A.* **72**, 2819–2823 (1975).

69. J. Hara *et al.*, Genetic ablation of orexin neurons in mice results in narcolepsy, hypophagia, and obesity. *Neuron* **30**, 345–354 (2001).

70. E. Coley, R. Farhadi, S. Lewis, I. R. Whittle, The incidence of seizures following Deep Brain Stimulating electrode implantation for movement disorders, pain and psychiatric conditions. *Br. J. Neurosurg.* **23**, 179–183 (2009).

71. T. J. Atchley *et al.*, Incidence and risk factors for seizures associated with deep brain stimulation surgery. *J. Neurosurg.* **135**, 279–283 (2020).

72. Y. Tan *et al.*, Impaired hypocretin/orexin system alters responses to salient stimuli in obese male mice. *J. Clin. Invest.* **130**, 4985–4998 (2020).

73. A. May *et al.*, Hypothalamic deep brain stimulation in positron emission tomography. *J. Neurosci.* **26**, 3589–3593 (2006).

74. J. A. González *et al.*, Inhibitory interplay between orexin neurons and eating. *Curr. Biol.* **26**, 2486–2491 (2016).

75. M. M. Karnani *et al.*, Role of spontaneous and sensory orexin network dynamics in rapid locomotion initiation. *Prog. Neurobiol.* **187**, 101771 (2020).

76. M. Fleischer, H. Endres, M. Sendtner, J. Volkmann, Development of a fully implantable stimulator for deep brain stimulation in mice. *Front. Neurosci.* **14**, 726 (2020).

77. D. E. Hardesty, H. A. Sackeim, Deep brain stimulation in movement and psychiatric disorders. *Biol. Psychiatry* **61**, 831–835 (2007).

78. C. Kosse, D. Burdakov, Natural hypothalamic circuit dynamics underlying object memorization. *Nat. Commun.* **10**, 1–8 (2019).

79. C. Concetti, E. F. Bracey, D. Peleg-Raibstein, D. Burdakov, Control of fear extinction by hypothalamic melanin-concentrating hormone-expressing neurons. *Proc. Natl. Acad. Sci. U.S.A.* **117**, 22514–22521 (2020).

80. C. K. Kim *et al.*, Simultaneous fast measurement of circuit dynamics at multiple sites across the mammalian brain. *Nat. Methods* **13**, 325–328 (2016).

81. S. Osawa *et al.*, Optogenetically induced seizure and the longitudinal hippocampal network dynamics. *PLoS One* **8**, e60928 (2013).

82. C. Touma, R. Palme, N. Sachser, Analyzing corticosterone metabolites in fecal samples of mice: A noninvasive technique to monitor stress hormones. *Horm. Behav.* **45**, 10–22 (2004).

83. K. S. Abelson, O. Kalliokoski, A. C. Teilmann, J. Hau, Applicability of commercially available ELISA kits for the quantification of faecal immunoreactive corticosterone metabolites in mice. *In Vivo* **30**, 739–744 (2016).

84. D. Peleg-Raibstein, J. Feldon, Differential effects of post-weaning juvenile stress on the behaviour of C57BL/6 mice in adolescence and adulthood. *Psychopharmacology (Berl.)* **214**, 339–351 (2011).

85. D. Peleg-Raibstein, E. Luca, C. Wolfrum, Maternal high-fat diet in mice programs emotional behavior in adulthood. *Behav. Brain Res.* **233**, 398–404 (2012).